Available online at www.sciencedirect.com
ScienceDirect
International Journal of Multiphase Flow 34 (2008) 176–187
International Journal of Multiphase Flow
www.elsevier.com/locate/ijmulflow

# Temporal stability of a particle-laden jet

T.L. Chan [a,*], F.B. Bao [a], J.Z. Lin [b], Y. Zhou [a], C.K. Chan [c]

[a] Department of Mechanical Engineering, The Hong Kong Polytechnic University, Hung Hom, Kowloon, Hong Kong
[b] China Jiliang University, Hangzhou 310018, China
[c] Department of Applied Mathematics, The Hong Kong Polytechnic University, Kowloon, Hong Kong

Received 2 August 2006; received in revised form 11 May 2007

**Abstract**

The temporal instability of a particle-laden jet was investigated numerically which took into consideration the parametric effects of jet parameter, $B$, jet Reynolds number, $Re_j$, particle mass loading, $Z$ and Stokes number, $St$. The linear stability theory was used to derive the instability equations of a viscous particle-laden jet flow. The single-phase instability of a top-hat jet was then calculated and compared with the available analytical theories. The numerical results agree well with the analytical results for both the axisymmetric ($n = 0$) and first azimuthal ($n = 1$) modes. The results show that the first azimuthal mode disturbance is usually more unstable than that of the axisymmetric mode. But the axisymmetric mode disturbance can be more unstable when $Z$ is high enough (i.e., $Z \geqslant 0.1$). The higher $B$ and $Re_j$ are, the more unstable the particle-laden jet will be. The existence of particles enhances the flow stability. With the increasing of $Z$, the jet flow will grow more stable. The inviscid single-phase jet is the most unstable. The wave amplification, $c_i$ first decreases with the increasing of $St$ and then increases afterwards. There exist certain values of $St$, at which the jet is the most stable.


*Keywords:* Particle-laden jet flow; Temporal instability; Stokes number; Particle mass loading

## 1. Introduction

Numerous engineering applications and processes of a two-phase turbulent jet for transporting particles can be identified (i.e., air cleaner systems, ejector scrubbers, air-spray systems, vehicular exhaust jet particle distributions and combustion exhaust systems, etc.). In many of these processes, the distribution of the dispersed particle is a controlling factor in the efficiency and the stability of the processes (Chan et al., 2005a,b, 2006; Lin et al., 2007). Since the stability of particle-laden jet flow is different from that of the single

* Corresponding author. Tel.: +852 2766 6656; fax: +852 2365 4703.
*E-mail address:* mmtlchan@inet.polyu.edu.hk (T.L. Chan).

0301-9322/$ - see front matter © 2007 Elsevier Ltd. All rights reserved.
doi:10.1016/j.ijmultiphaseflow.2007.10.002

phase jet flow (Saffman, 1962; Batchelor and Gill, 1962), it plays a key role in the numerous engineering applications and processes.

Indeed, Batchelor and Gill (1962) derived the coupled ordinary differential equations for the disturbance motion of a single-phase jet and proved the existence of amplified disturbance for any value of the azimuthal wavenumber for a top-hat velocity profile. Lessen and Singh (1973) studied both temporal and spatial instability of axisymmetric free shear layers and concluded that the first azimuthal mode is the most unstable. Mollendorf and Gebhart (1973) solved numerically the fully viscous hydrodynamic stability equations for a laminar vertical round jet for both symmetric and asymmetric disturbances using the proper boundary-layer base-flow velocity profile. Michalke (1984) reviewed the theoretical results on the instability of axisymmetric jets due to the effects of shear layer thickness, Mach number, temperature ratio and external flow velocity. Lin and Lian (1989) studied the effect of the ambient gas density on the onset of absolute instability in a viscous liquid jet. They found that the critical Weber number can be determined as a function of Reynolds number and the density ratio of gas to liquid. Shen and Li (1996) carried out a linear analysis for the temporal instability of an annular viscous liquid jet moving in an inviscid gas medium. They found that the curvature effects in general increase the disturbance growth rate and an ambient gas medium always enhances the annular jet instability. Recently, Cramer et al. (2002) have studied experimentally the breakup of a Newtonian liquid jet into droplets injected horizontally into another flowing immiscible Newtonian fluid under creeping flow conditions. They have found that different breakup mechanisms take place in different flow regions. Funada et al. (2004) have analyzed the temporal and convective/absolute instability of a liquid jet into a gas or another liquid medium using viscous potential flow. Their findings have showed that there are wavenumbers for which the liquid jet is temporally unstable for their studied parameters. Chauhan et al. (2006) have examined the emergence of the absolute instability from the convectively unstable states of an inviscid compound jet. They have found that in addition to being convectively unstable at all Weber numbers, the inviscid compound jet is also absolutely unstable when below its critical velocity.

On the other hand, the instability studies of a particle-laden jet have also been developed. Neglecting the gas viscosity and the fluctuation of suspension velocity, Yang et al. (1990) studied the spatial stability of gas-particle two-phase mixing layer. They found that the existence of small particles enhances the flow stability. Sykes and Lyell (1994) investigated the spatial stability of an inviscid two-phase circular jet and also found that the particles have a stabilizing effect. The spatial growth rate was found to decrease for both the axisymmetric and first azimuthal modes. Parthasarathy (1995) studied both the spatial and temporal stabilities of a circular particle-laden jet. The temporal stability analysis of a particle-laden top-hat jet showed that the presence of particles decreases the wave amplification but increases the wave velocity. However, the increasing of particle mass loading decreases both wave amplification and velocity. The spatial stability analysis showed that the presence of particles decreases the wave amplification rate at all frequencies. However, only top-hat jet profile was investigated in the temporal instability. Recently, Lin and Zhou (2000) have investigated the stability of a moving jet containing dense suspended solid particles and found that the particles affect the instability of the flow field significantly. DeSpirito and Wang (2001) have studied the temporal stability of a particle-laden jet using the direct numerical simulation approach. They have demonstrated that the addition of particles can destabilize the flow at a small particle Stokes number, while the stabilizing effect prevails for an intermediate to a large particle Stokes number. The addition of particles increases the wave velocity at high wavenumber but decreases the wave velocity at low wavenumber. For a given particle mass loading and wavenumber, there is an intermediate particle Stokes number that corresponds to a maximum stability of jet flow. They have showed that this Stokes number is on the order of 1 and depends weakly on the wavenumber. But they have only considered the axisymmetric azimuthal mode disturbance. In fact, the first azimuthal mode disturbance is more unstable. Lakehal and Narayanan (2003) have studied the initial temporal evolution of mixing layers for different Stokes numbers. Their results could also apply for the instability of jet flow.

However, there is no detailed investigation on different azimuthal modes in the instability of a particle-laden jet which takes into consideration the different parametric effects available in the literature. In the present study, it is intended to investigate the parametric effects of jet parameter, $B$, jet Reynolds number, $Re_j$, particle mass loading, $Z$, particle Stokes number, $St$, disturbance wavenumber, $\beta$ and azimuthal mode, $n$ on the temporal stability of a particle-laden jet.

## 2. Stability equations and boundary conditions

### 2.1. Stability equations

The volume fraction of particulate phase in an axisymmetric gas jet shear layer containing solid particles is very low. Hence, the effects of particle concentrations on continuous phase viscosity are small, as described in DeSpirito and Wang (2001). The diameter sizes of particles considered are from about 1 to 100 μm. These studied diameter sizes of particles are much smaller than any characteristic length scales of the gas flow. The particle density is much higher than that of the gas, so the bulk particle mass loading of the solid phase is on the order of 1. Because of its large density ratio, the effects of virtual mass, Basset history forces, etc., can be neglected. Since the particle Reynolds numbers are in the Stokes flow region, a linear Stokes drag is assumed (Saffman, 1962; Parthasarathy, 1995 and DeSpirito and Wang, 2001). The governing equations for the carrier gas (subscript f) and the solid phase (subscript p) of an axisymmetric jet are:

$$\frac{\partial \boldsymbol{u}}{\partial t} + \boldsymbol{u}\cdot\nabla\boldsymbol{u} = -\frac{1}{\rho_{\mathrm{f}}}\nabla p + \frac{\mu}{\rho_{\mathrm{f}}}\nabla^2\boldsymbol{u} - \frac{3\pi\mu N d}{\rho_{\mathrm{f}}}(\boldsymbol{u}-\boldsymbol{v}), \tag{1}$$

$$\nabla\cdot\boldsymbol{u} = 0, \tag{2}$$

$$\frac{\partial \boldsymbol{v}}{\partial t} + \boldsymbol{v}\cdot\nabla\boldsymbol{v} = \frac{18\mu}{\rho_{\mathrm{p}} d^2}(\boldsymbol{u}-\boldsymbol{v}), \tag{3}$$

$$\frac{\partial \alpha}{\partial t} + \nabla\cdot(\alpha\boldsymbol{v}) = 0, \tag{4}$$

where $\boldsymbol{u} = (u_r, u_\theta, u_z)$ is the gas velocity; $\boldsymbol{v} = (v_r, v_\theta, v_z)$ is the particle velocity; $p$ is the gas pressure; $\rho_{\mathrm{f}}$ is the gas density; $\rho_{\mathrm{p}}$ is the particle density. The momentum coupling is described by the term $3\pi\mu N d(\boldsymbol{u}-\boldsymbol{v})$, where $N$ is the particle number density; $d$ is the particle diameter; $\mu$ and $v$ are the gas dynamic and kinematic viscosity, respectively (Saffman, 1962). The local particle volume fraction, $\alpha$ is related to the number density as $\alpha = N\pi d^3/6$.

The governing equations, Eqs. (1)–(4) can be non-dimensionalized using the gas velocity at the centerline of the jet, $U_0$, the radius of the jet core, $r_0$, and an average particle volume fraction, $\alpha_0$. A linear stability analysis is performed by separating the variables into the mean and perturbation components as:

$$\boldsymbol{u} = \boldsymbol{U} + \boldsymbol{u}', \quad \boldsymbol{v} = \boldsymbol{V} + \boldsymbol{v}', \quad p = P + p', \quad \alpha = A + \alpha', \tag{5}$$

where the primed ($'$) variables are the perturbation components; $U$ and $V$ are the steady mean velocity of gas and particle, respectively; $P$ is the steady mean pressure; $A$ is the normalized average particle volume fraction and is equal to 1. For the sufficiently fine particles, the velocity of sedimentation will be small compared with a characteristic velocity of the flow and hence it can be neglected (Saffman, 1962). The inertial force is small compared to the viscosity force. The particle moves along the flow streamline. The mean velocity of particles can be considered as the behavior of gas flow as used in Batchelor and Gill (1962), Saffman (1962) and DeSpirito and Wang (2001). In the jet flow, the jet velocity can be considered as a parallel flow and thus $\boldsymbol{U} = \boldsymbol{V} = \{0, 0, U\}$. Eq. (5) is substituted into nondimensional forms of Eqs. (1)–(4). When the mean flow terms are subtracted and the nonlinear terms of the perturbation are neglected, the linear stability equations can then be expressed as:

$$\frac{\partial \boldsymbol{u}'}{\partial t} + (\boldsymbol{u}'\cdot\nabla)\boldsymbol{U} + (\boldsymbol{U}\cdot\nabla)\boldsymbol{u}' = -\nabla p' + \frac{1}{Re_{\mathrm{j}}}\nabla^2\boldsymbol{u}' - \frac{Z}{St}(\boldsymbol{u}'-\boldsymbol{v}'), \tag{6}$$

$$\nabla\cdot\boldsymbol{u}' = 0, \tag{7}$$

$$\frac{\partial \boldsymbol{v}'}{\partial t} + (\boldsymbol{v}\cdot\nabla)\boldsymbol{U} + (\boldsymbol{U}\cdot\nabla)\boldsymbol{v} = \frac{1}{St}(\boldsymbol{u}'-\boldsymbol{v}'), \tag{8}$$

$$\frac{\partial \alpha'}{\partial t} + \nabla\cdot(\boldsymbol{v}' + \alpha'\boldsymbol{U}) = 0. \tag{9}$$

The jet flow Reynolds number, $Re_j$ is defined as $r_0 U_0/v$. In the flow momentum coupling term, $Z$ is the average particle mass loading ($Z = \alpha_0 \rho_p/\rho_f$); the particle Stokes number, $St$ is the ratio of the particle response time ($\tau_p = \rho_p d^2/18 v \rho_f$) to flow characteristic time ($\tau_f = r_0/U_0$).

The perturbations are described as the normal mode of a traveling wave form:

$$\frac{u_r'}{\mathrm{i}u_r(r)} = \frac{u_\theta'}{u_\theta(r)} = \frac{u_z'}{u_z(r)} = \frac{v_r'}{\mathrm{i}v_r(r)} = \frac{v_\theta'}{v_\theta(r)} = \frac{v_z'}{v_z(r)} = \frac{p'}{p(r)} = \exp(\mathrm{i}n\theta + \mathrm{i}\beta(x - ct)), \tag{10}$$

where $u(r)$, $v(r)$ and $p(r)$ are the amplitudes of the corresponding disturbances; $n$ is the azimuthal mode of disturbance; $\beta$ is the axial wavenumber of disturbance; $c$ is the wave amplification factor; $u_r$ is taken to be directly proportional to $\mathrm{i}u_r(r)$ due to the phase of $u_r$ differs by $\pi/2$ from that of $u_\theta$ and $u_z$ as well as $v_r$ in Eq. (7) (Batchelor and Gill, 1962; Saffman, 1962).

In the present study, the temporal instability of a particle-laden jet is considered. Hence, $\beta$ is real quantity while $c = c_r + \mathrm{i}c_i$ is generally complex. The disturbances will grow with time if $c_i > 0$ and will decay if $c_i < 0$ in Eq. (10). The neutral disturbances are then characterized by $c_i = 0$. Substituting Eq. (10) into Eqs. (6)–(9), they can be expressed as:

$$\begin{aligned}
&\beta^3(U-c)u_\theta + \frac{n}{r}\beta(U-c)\left(D_* u_r + \frac{n}{r}u_\theta\right) - \frac{n}{r}\beta u_r DU \\
&\quad = \mathrm{i}\frac{Z}{St}\left(\frac{n}{r}D_* u_r + \left(\beta^2 + \frac{n^2}{r^2}\right)u_\theta - \beta^2 v_\theta + \frac{n}{r}\beta v_z\right) - \frac{\mathrm{i}}{Re_j}\left(\beta^2\left(DD_* - \beta^2 - \frac{n^2}{r^2}\right)u_\theta - \frac{2n}{r^2}\beta^2 u_r\right. \\
&\qquad \left. + \frac{n}{r}\left(D_* D - \beta^2 - \frac{n^2}{r^2}\right)\left(D_* u_r + \frac{n}{r}u_\theta\right)\right),
\end{aligned} \tag{11}$$

$$\begin{aligned}
&-\beta^3(U-c)u_r + \beta D\left((U-c)\left(D_* u_r + \frac{n}{r}u_\theta\right)\right) - \beta D(u_r DU) \\
&\quad = \mathrm{i}\frac{Z}{St}\left((DD_* - \beta^2)u_r + D\left(\frac{n}{r}u_\theta\right) + \beta^2 v_r + \beta D v_z\right) - \frac{\mathrm{i}}{Re_j}\left(D\left(\left(D_* D - \beta^2 - \frac{n^2}{r^2}\right)\left(D_* u_r + \frac{n}{r}u_\theta\right)\right)\right. \\
&\qquad \left. - \left(DD_* - \beta^2 - \frac{n^2}{r^2}\right)\beta^2 u_r + \frac{2n}{r^2}\beta^2 u_\theta\right),
\end{aligned} \tag{12}$$

$$\mathrm{i}\beta(U-c)v_r = \frac{1}{St}(u_r - v_r), \tag{13}$$

$$\mathrm{i}\beta(U-c)v_\theta = \frac{1}{St}(u_\theta - v_\theta), \tag{14}$$

$$\mathrm{i}\beta(U-c)v_z + \mathrm{i}v_r DU = \frac{1}{St}(u_z - v_z), \tag{15}$$

$$\beta(U-c)\alpha + \left(D_* v_r + \frac{n}{r}v_\theta + \beta v_z\right) = 0, \tag{16}$$

where the differential operations $D$ and $D_*$ are defined as:

$$D() = \frac{\mathrm{d}}{\mathrm{d}r}(), D_*() = \frac{\mathrm{d}}{\mathrm{d}r}() + \frac{1}{r}(). \tag{17}$$

The variable $\alpha$ only appears in Eq. (16) and it can be decoupled with other equations, Eqs. (11)–(15). Hence, Eqs. (11)–(15) form a closed eigenvalue problem together with the appropriate boundary conditions in Section 2.2.

### 2.2. Boundary conditions

The boundary conditions are set for different azimuthal modes. The following boundary conditions of disturbance were first derived by Batchelor and Gill (1962) and then adopted by many researchers (Lessen and Singh, 1973; Mollendorf and Gebhart, 1973; Morris, 1976; Michalke and Hermann, 1982). The boundary conditions of particle disturbance follow that of the gas phase. Hence, the boundary conditions used for the present study are:

$n = 0$:

$$u_r(0) = u_\theta(0) = Du_z(0) = Dp(0) = 0, \tag{18}$$
$$u_r(\infty) = u_\theta(\infty) = u_z(\infty) = p(\infty) = 0.$$

$n = 1$:

$$u_r(0) + u_\theta(0) = u_z(0) = p(0) = 0, \tag{19}$$
$$u_r(\infty) = u_\theta(\infty) = u_z(\infty) = p(\infty) = 0.$$

## 3. Jet velocity profile

The normalized jet velocity profile, $U$ has been widely used for the study of jet instability (Morris, 1976; Michalke, 1984; Sykes and Lyell, 1994 and Parthasarathy, 1995) as follows:

$$U = \frac{1}{2}\left(1 - \tanh\left(\frac{B}{4}\left(r - \frac{1}{r}\right)\right)\right), \tag{20}$$

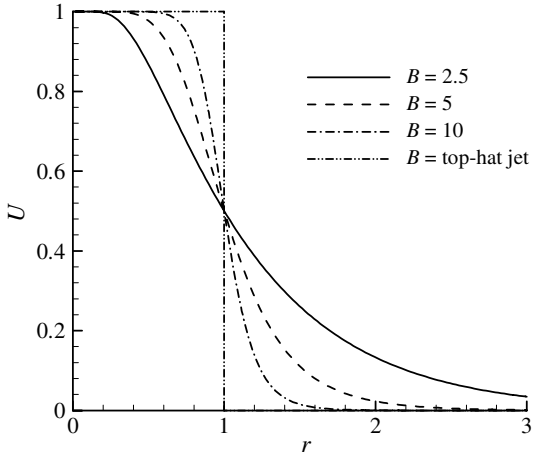


Fig. 1. Normalized velocity profiles for different jet parameter, $B$ and top-hat jet.

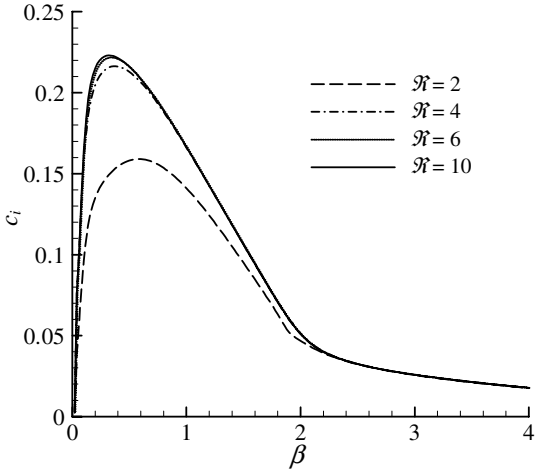


Fig. 2. Wave amplification, $c_i$ of a single jet as a function of wavenumber, $\beta$ for different domain size, $\Re$.

where $B$ is the jet parameter, $B = \frac{R}{\theta}$ where $R$ is the middle of the jet shear layer and $\theta$ is the momentum boundary layer thickness of the jet shear layer, $\theta = \int_0^\infty \left[\frac{u-u_\infty}{u_j-u_\infty}\right]\left[1-\frac{u-u_\infty}{u_j-u_\infty}\right] dr$, in which $u_j$ is the jet core velocity, $u_\infty$ is the external flow velocity. It is used to characterize jet velocity profiles for different axial locations. The smaller $B$ values, the farther downstream the locations. The normalized jet velocity profiles for different $B$ values and top-hat jet are shown in Fig. 1.

Although the outer boundary of the jet is located at infinity ($r = \infty$), it should be truncated at some finite values in the present numerical simulation. This finite domain size is denoted by $r = \Re$. The wave amplifications, $c_i$ of a single jet for $\Re$ ranging from 2 to 10 are shown in Fig. 2. It shows that the wave amplification of jet at $\Re = 6$ is almost the same trend as that of $\Re = 10$. It can also be concluded that $\Re = 6$ is far away enough for the outer boundary of an axisymmetric jet flow. Hence, the outer boundary is defined at $\Re = 6$ in the present study.

## 4. Results and discussions

### 4.1. Top-hat jet instability

The instability of a single-phase top-hat jet was solved completely by Batchelor and Gill (1962). The wave velocity, $c_r$ and wave amplification, $c_i$ for a growing disturbance are:

$$c_r = \frac{1}{1+L_n(\beta)}, \quad c_i = \frac{L_n^{\frac{1}{2}}(\beta)}{1+L_n(\beta)}, \tag{21}$$

where $L_n(\beta) = -\frac{K_n(\beta)I_n'(\beta)}{I_n(\beta)K_n'(\beta)}$, and $I_n$ and $K_n$ stand for the modified Bessel functions of the first and second kinds. The values of $c_r$ and $c_i$ as the functions of wavenumber, $\beta$ for different azimuthal modes, $n$ are shown in Fig. 3. The present numerical results are compared with the analytical results of Batchelor and Gill (1962) in order to validate the present developed numerical codes for solving eigenvalue problems. Excellent agreement on both the axisymmetric and first azimuthal modes is obtained.

### 4.2. Jet parameter effect

The effect of jet parameter, $B$ on its instability was first investigated. The variation of wave amplification, $c_i$ with wavenumber, $\beta$ for different $B$ and azimuthal modes, $n$ are shown in Fig. 4. It shows that the larger $B$ is, the more unstable jet will be, which is true for both $n = 0$ and 1 modes. When $B$ is higher, the normalized jet

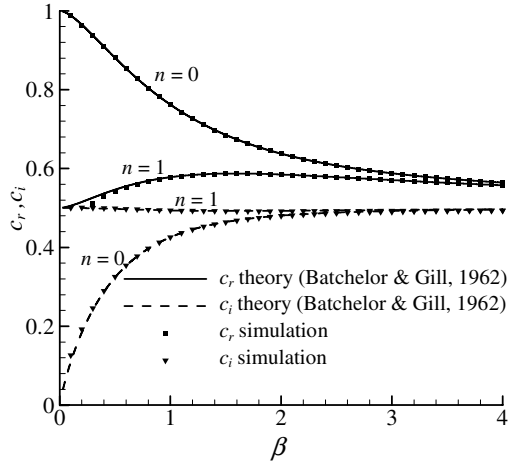


Fig. 3. Comparison of numerical results and Batchelor and Gill's theory (1962) for a top-hat jet for different azimuthal modes.

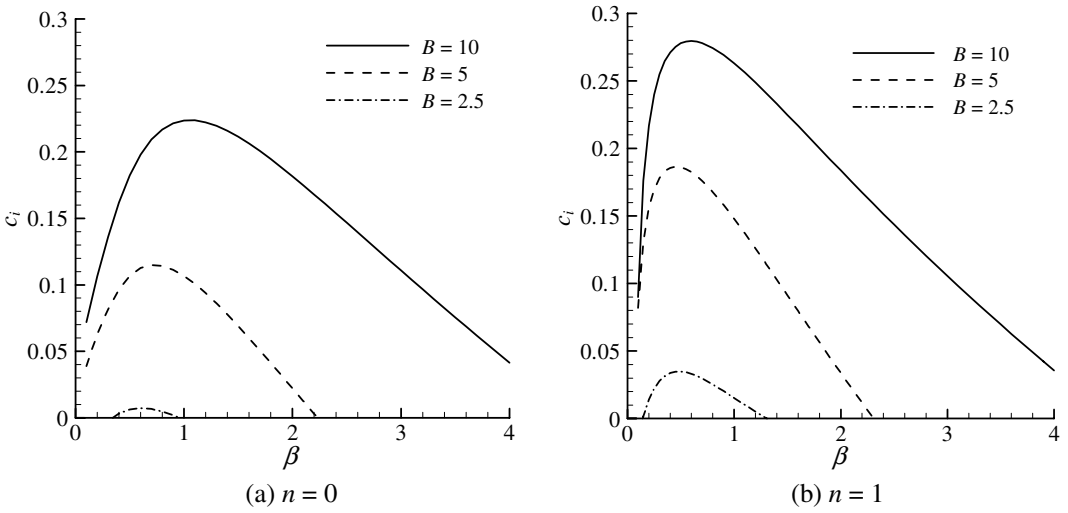


Fig. 4. Variation of wave amplification, $c_i$ with wavenumber, $\beta$ for different jet parameters, $B$: (a) $n = 0$; (b) $n = 1$ where $Re_j = 1000$, $Z = 0.01$ and $St = 1$.

velocity changes more sharply from 1 of the jet core to 0 of the ambient velocity, as shown in Fig. 1. It causes the larger shear force and leads the jet to be more unstable.

Fig. 4a and b show that the first azimuthal disturbance ($n = 1$) is more unstable than the axisymmetric azimuthal disturbance ($n = 0$), which can also be found in Fig. 3 for the top-hat jet. Similar findings were also reported by the researchers for the stability of a single-phase jet (Lessen and Singh, 1973; Michalke, 1984). With the increasing of $\beta$, $c_i$ increases first and then decreases accordingly. There exists the highest $c_i$ at certain $\beta$ value (i.e., $\beta = 0.7$ when $B = 5$). At this $\beta$ value, the particle-laden jet is the most unstable. In general, the corresponding $\beta$ to the highest $c_i$ increases in respect to $B$, which is true for both $n = 0$ and 1 modes. When $n = 0$, the corresponding $\beta$ to the highest $c_i$ for $B$ from 2.5 to 10 is about 0.6–1, which is higher than that of $n = 1$ for about 0.4–0.6.

The variation of $c_i$ and $c_r$ in respect to $B$ for both axisymmetric and first azimuthal modes is shown in Fig. 5. The $c_i$ increases with the increasing of $B$. Similar numerical results were found in DeSpirito and Wang (2001). The first azimuthal mode is more unstable than the axisymmetric mode. The $c_r$ decreases with $B$ first and then tends to have different constant trends for both $n = 0$ and 1 modes.

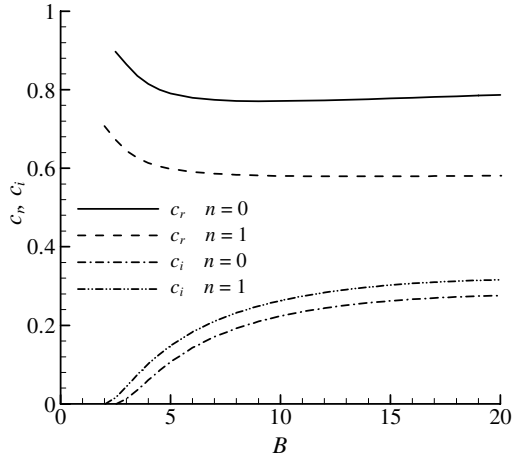


Fig. 5. Behavior of wave amplification, $c_i$ and velocity, $c_r$ with jet parameter, $B$ for different azimuthal modes, $n$, where $Re_j = 1000$, $Z = 0.01$, $St = 1$ and $\beta = 1$.

### 4.3. Jet Reynolds number effect

The variation of wave amplification, $c_i$ with the wavenumber, $\beta$ for different jet Reynolds numbers ($Re_j = 100$, 500 and 2000) and inviscid case for different azimuthal modes, $n$ is shown in Fig. 6. It shows that for both $n = 0$ and 1 modes, the higher $Re_j$ is, the more unstable the jet will be. The $c_i$ gradually approaches to the inviscid solution as $Re_j$ increases. The instable region of $\beta$ also increases with the increasing of $Re_j$. Comparing with Fig. 6a and b, the first azimuthal mode is more unstable than the axisymmetric azimuthal mode. The corresponding $\beta$ to the highest $c_i$ decreases with the increasing of $Re_j$, which is true for both $n = 0$ and 1 modes. When $n = 0$, the corresponding $\beta$ to the highest $c_i$ for $Re_j$ from 100 to 2000 is about 0.6–0.9, which is larger than that of $n = 1$ for 0.4–0.7.

The effect of $Re_j$ on the stability of a single-phase jet and a particle-laden jet for different azimuthal modes, $n$ is shown in Fig. 7. Both types of jets grow unstable and approach the inviscid solution as $Re_j$ increases. The

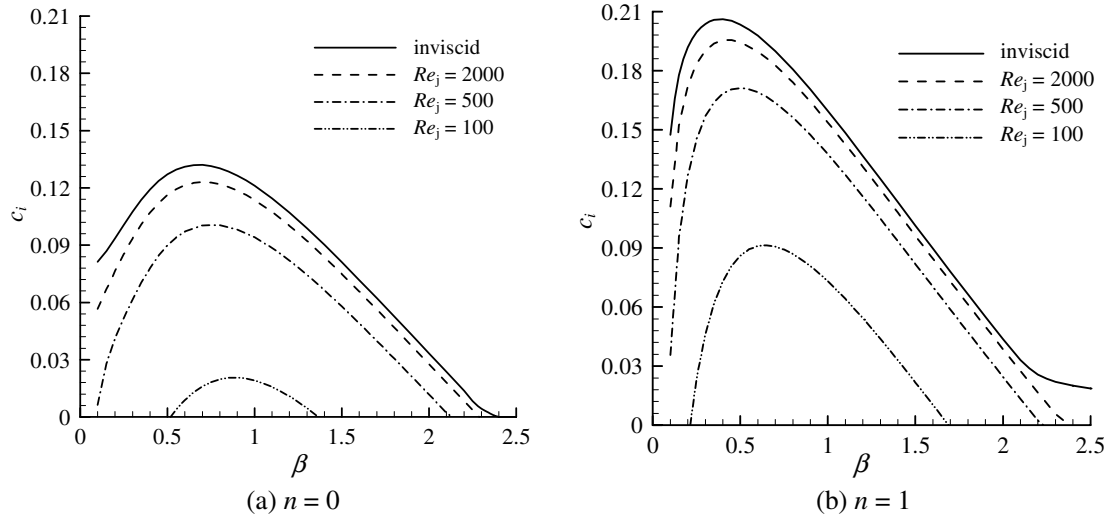


Fig. 6. Wave amplification, $c_i$ as a function of wavenumber, $\beta$ for different jet Reynolds numbers, $Re_j$: (a) $n = 0$; (b) $n = 1$ where $B = 5$, $Z = 0.01$ and $St = 1$.

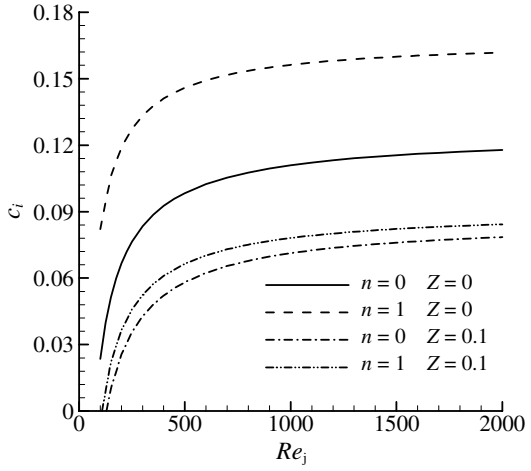


Fig. 7. Wave amplification, $c_i$ as a function of jet Reynolds number, $Re_j$ for different particle mass loadings, $Z$ and azimuthal modes, $n$, where $B = 5$, $St = 1$ and $\beta = 1$.

particle-laden jet is more stable than the single-phase jet for both $n = 0$ and 1 modes, which will be discussed in Section 4.4.

### 4.4. Particle mass loading effect

The variation of wave amplification, $c_i$ with wavenumber, $\beta$ for different particle mass loadings, $Z$ and azimuthal modes, $n$ are shown in Fig. 8. It shows that the higher $Z$ is, the more stable the jet will be, which is true for both $n = 0$ and 1 modes. The existence of particles assists the stability of jet flow. It demonstrates that the single-phase jet is the most unstable. For the studied jet parameter, $B$ and jet Reynolds number, $Re_j$, the particle-laden jet is always stable when $Z$ is high enough (i.e., $Z > 1$). When $Z$ is small (i.e., $Z = 0.02$), the first azimuthal mode is more unstable than the axisymmetric azimuthal mode. On the other hand, when $Z$ is higher (i.e., $Z \geqslant 0.1$), the axisymmetric azimuthal mode can be more unstable than the first azimuthal mode, which can be found in Figs. 8 and 9.

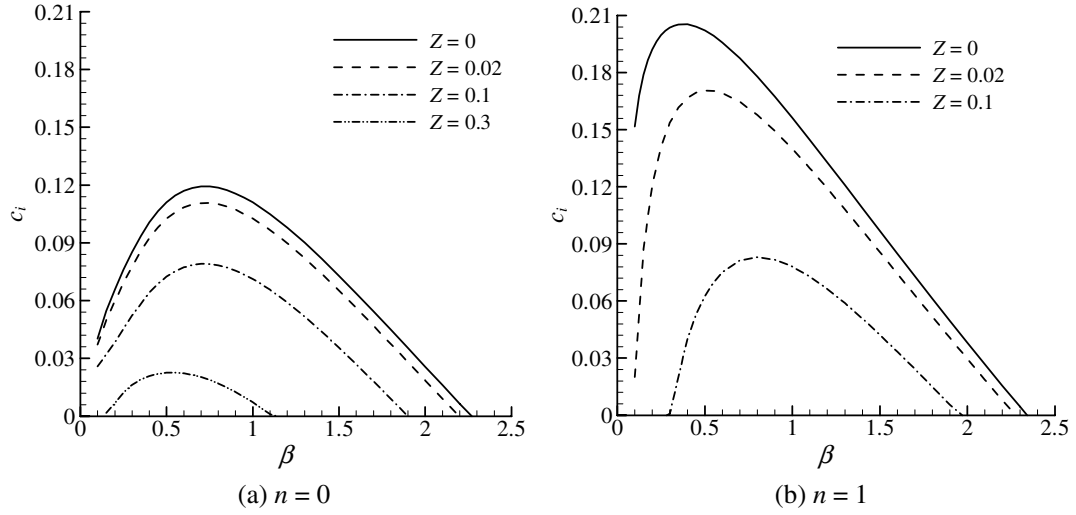


Fig. 8. Wave amplification, $c_i$ as a function of wavenumber, $\beta$ for different particle mass loadings, $Z$: (a) $n = 0$; (b) $n = 1$ where $B = 5$, $Re_j = 1000$, and $St = 1$.

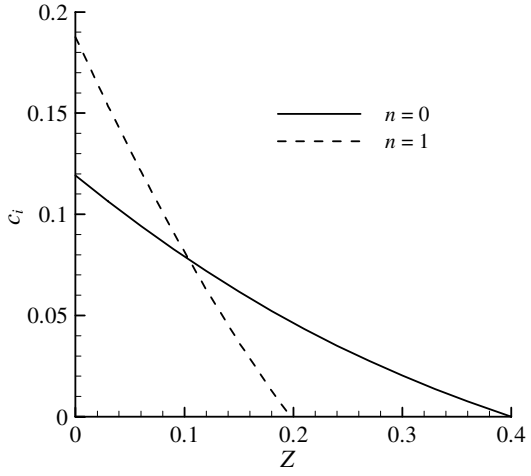


Fig. 9. Variation of wave amplification, $c_i$ with particle mass loading, $Z$ for different azimuthal modes, $n$, where $B = 5$, $Re_j = 1000$, $St = 1$ and $\beta = 0.7$.

The corresponding $\beta$ to the maximum $c_i$ changes significantly for the particle mass loading for $n = 0$ and 1 modes as shown in Fig. 8. When $n = 0$, the corresponding $\beta$ decreases with the increasing of $Z$, from 0.8 to 0.5, while for $n = 1$, the corresponding $\beta$ increases with the increasing of $Z$ from 0.4 to 0.8.

The effect of $Z$ on the instability of jet for different azimuthal modes, $n$ is shown in Fig. 9. The $c_i$ decreases with the increasing of $Z$. The effect is much more obvious for the first azimuthal mode $n = 1$. At small $Z$, the $n = 1$ is more unstable than the $n = 0$, but when $Z$ is higher than 0.1, this phenomena will be vice versa.

### 4.5. Particle Stokes number effect

The effect of particle Stokes number, $St$ on the stability of a particle-laden jet for different jet Reynolds numbers, $Re_j$ is shown in Fig. 10. For the studied $Re_j$, with the increasing of $St$ from 0.01 to 100, $c_i$ decreases first and then increases accordingly. The minimum $c_i$ appears when $St$ is at the order of 1, which also agrees well with the findings of DeSpirito and Wang (2001). When $St > 1$, almost the same $c_i$ is found for the studied $Re_j$. The $c_i$ tends to be at inviscid flow situation when $Re_j$ is higher than 2000, as shown in Fig. 7. However, different phenomenon are found when $St < 1$.

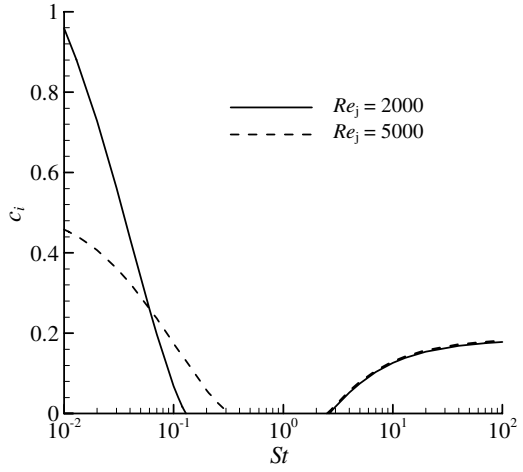


Fig. 10. Variation of wave amplification, $c_i$ with particle Stokes number, $St$ for different jet Reynolds numbers, $Re_j$, where $B = 5$, $n = 1$, $Z = 0.5$ and $\beta = 0.8$.

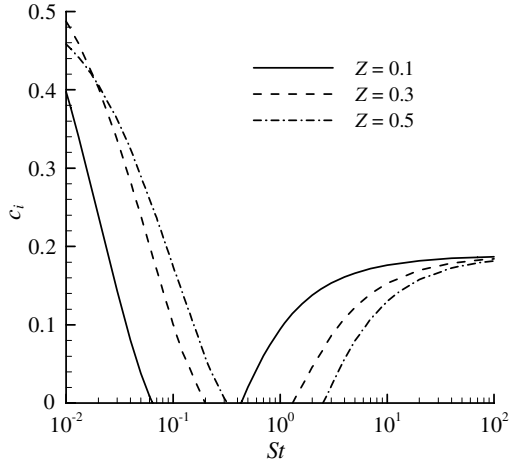


Fig. 11. Variation of wave amplification, $c_i$ with particle Stokes number, $St$ for different particle mass loadings, $Z$ where $B = 5$, $n = 1$, $Re_j = 5000$ and $\beta = 0.8$.

The effect of $St$ on the stability of a particle-laden jet for different $Z$ is shown in Fig. 11. For the studied $Z$, with the increase of $St$ from 0.01 to 100, $c_i$ decreases first and then increases accordingly. The corresponding $St$ to the minimum $c_i$ is different for different $Z$. When $Z = 0.5$, the corresponding $St$ is about 1, but when $Z = 0.1$, the corresponding $St$ is about 0.1.

## 5. Conclusions

The temporal instability of a particle-laden jet was investigated numerically which took into consideration the parametric effects of jet parameter, $B$, jet Reynolds number, $Re_j$, particle mass loading, $Z$ and Stokes number, $St$. The instability equations of a viscous particle-laden jet flow were first derived using the linear stability theory. The instability of a single phase top-hat jet was then calculated and compared with the analytical theories. The numerical results agree well with the analytical results for both the axisymmetric ($n = 0$) and first azimuthal ($n = 1$) modes. The axisymmetric and first azimuthal mode disturbances have the same tendency for different studied cases. The results show that the first azimuthal mode disturbance is usually more unstable than the axisymmetric mode disturbance, which is usually true for studied parametric effects. If $Z$ is high enough (i.e., $Z \geqslant 0.1$), then the axisymmetric mode is more unstable than the first azimuthal mode. With the increasing of wavenumber, $\beta$, the wave amplification, $c_i$ first increases and then decreases accordingly. There exists a maximum $c_i$ which corresponds to $\beta$ at about 0.5–1. The corresponding $\beta$ increases with increasing of $B$ but decreases with increasing of $Re$ for both $n = 0$ and 1 modes. But the corresponding $\beta$ decreases with the increasing of $Z$ for $n = 0$, while the corresponding $\beta$ increases with the increasing of $Z$ for $n = 1$. The higher $B$ and $Re_j$ are, the more unstable the particle-laden jet will be. With the increasing of $Z$, the jet flow will grow more stable. The inviscid single-phase jet is the most unstable. The wave amplification, $c_i$ first decreases with the increasing of $St$ and then increases afterwards. There exist certain values of $St$, at which the jet is the most stable.

## Acknowledgements

This work was supported by the Grant from the Central Research Grants of The Hong Kong Polytechnic University (Project No. A-PA2V). The authors would like to thank the valuable discussions and suggestions from Prof. L.P. Wang and Dr. J. DeSpirito on the development of present work.

## References

Batchelor, G.K., Gill, A.E., 1962. Analysis of the stability of axisymmetric jets. J. Fluid Mech. 14, 529–551.

Chan, T.L., Zhou, K., Lin, J.Z., Liu, C.H., 2005a. Large eddy simulation of fluid flow and gas-to-nanoparticle conversion and distribution of a moving vehicle in urban road microenvironments. Paper presented at The Second International Conference for Mesoscopic Methods in Engineering and Science, 26–29 July 2005, Hong Kong. ISBN 962-367-475-9.

Chan, T.L., Zhou, K., Lin, J.Z., 2005b. Modeling study of gas-to-nanoparticle conversion from a vehicular exhaust plume. Paper No. P-124. In: Proceedings of International Conference on Jets, Wakes and Separated Flows, ICJWSF-2005, 5–8 October 2005, Toba-shi, Mie, Japan.

Chan, T.L., Lin, J.Z., Zhou, K., Chan, C.K., 2006. Simultaneous numerical simulation of nano and fine particle coagulation and dispersion in a round jet. J. Aerosol Sci. 37, 1545–1561.

Chauhan, A., Maldarelli, C., Papageorgiou, D.T., Rumschtzki, D.S., 2006. The absolute instability of an inviscid compound jet. J. Fluid Mech. 549, 81–98.

Cramer, C., Beruter, B., Fischer, P., Windhab, E.J., 2002. Liquid jet stability in a laminar flow field. Chem. Eng. Technol. 25, 499–506.

DeSpirito, J., Wang, L.P., 2001. Linear instability of two-way coupled particle-laden jet. Int. J. Multiphase Flow 27, 1179–1198.

Funada, T., Joseph, D.D., Yamashita, S., 2004. Stability of a liquid jet into incompressible gases and liquids. Int. J. Multiphase Flow 30, 1279–1310.

Lakehal, D., Narayanan, C., 2003. Numerical analysis of the continuum formulation for the initial evolution of mixing layers with particles. Int. J. Multiphase Flow 29, 927–941.

Lessen, M., Singh, P.J., 1973. The stability of axisymmetric free shear layers. J. Fluid Mech. 60, 433–457.

Lin, J.Z., Zhou, Z.X., 2000. Research on stability of moving jet containing dense suspended solid particles. Appl. Math. Mech. 21, 1390–1400 (English edition).

Lin, J.Z., Chan, T.L., Liu, S., Zhou, K., Zhou, Y., Lee, S.C., 2007. Effects of coherent structures on nanoparticle coagulation and dispersion in a round jet. Int. J. Nonlinear Sci. Numer. Simul. 8, 45–54.

Lin, S.P., Lian, Z.W., 1989. Absolute instability of a liquid jet in a gas. Phys. Fluids 1, 490–493.
Michalke, A., 1984. Survey on jet instability theory. Prog. Aerosp. Sci. 21, 159–199.
Michalke, A., Hermann, G., 1982. On the inviscid instability of a circular jet with external flow. J. Fluid Mech. 114, 343–359.
Mollendorf, J.C., Gebhart, B., 1973. An experimental and numerical study of the viscous stability of a round laminar vertical jet with and without thermal buoyancy for symmetric and asymmetric disturbances. J. Fluid Mech. 61, 367–399.
Morris, P.J., 1976. The spatial viscous instability of axisymmetric jets. J. Fluid Mech. 77, 511–529.
Parthasarathy, R.N., 1995. Stability of particle-laden round jets to small disturbances. Trans. ASME 228, 427–434.
Saffman, P.G., 1962. On the stability of laminar flow of a dusty gas. J. Fluid Mech. 13, 120–128.
Shen, J., Li, X., 1996. Instability of an annular viscous liquid jet. Acta Mech. 114, 167–183.
Sykes, D., Lyell, M.J., 1994. The effect of particle loading on the spatial stability of a circular jet. Phys. Fluids 6, 1937–1939.
Yang, Y.Q., Chung, J.N., Troutt, T.R., Crowe, C.T., 1990. The influence of particles on the spatial stability of two phase mixing layers. Phys. Fluids A2, 1839–1845.